

Author Manuscript

This is the author manuscript accepted for publication and has undergone full peer review but has not been through the copyediting, typesetting, pagination and proofreading process, which may lead to differences between this version and the [Version of Record](#). Please cite this article as [doi: 10.1002/ECM.1355](https://doi.org/10.1002/ECM.1355)

This article is protected by copyright. All rights reserved

1 Spatially-structured statistical network models for
2 landscape genetics

3 Running Head: Estimating resistance parameters

4
5 Erin E. Peterson^{1*}, Ephraim M. Hanks², Mevin B. Hooten³,
Jay M. Ver Hoef⁴, and Marie-Josée Fortin⁵

¹ ARC Centre for Excellence in Mathematical and
Statistical Frontiers (ACEMS) and the Institute for Future Environments,
Queensland University of Technology (QUT),
Brisbane, QLD, 4000, Australia

² Department of Statistics, Pennsylvania State University,
University Park, PA, 16801, USA

³ U.S. Geological Survey, Colorado Cooperative Fish and Wildlife Research Unit,
Department of Fish, Wildlife, and Conservation Biology,
and Department of Statistics,
Colorado State University, Fort Collins, CO, 80523, USA

⁴ Marine Mammal Laboratory,
NOAA-NMFS Alaska Fisheries Science Center,
Seattle, WA, 98115, USA

⁵ Department of Ecology & Evolutionary Biology
University of Toronto, Toronto, ON, Canada

*Corresponding Author Email: Erin.Peterson@qut.edu.au

6 January 7, 2019

7 **Abstract**

8 A basic understanding of how the landscape impedes, or creates resistance
9 to, the dispersal of organisms and hence gene flow is paramount for successful
10 conservation science and management. Spatially structured ecological networks
11 are often used to represent spatial landscape-genetic relationships, where nodes
12 represent individuals or populations and resistance to movement is represented
13 using non-binary edge weights. Weights are typically assigned or estimated by
14 the user, rather than observed, and validating such weights is challenging. We
15 provide a synthesis of current methods used to estimate edge weights and an
16 overview of common model types, stressing the advantages and disadvantages of
17 each approach and their ability to model landscape-genetic data. We further
18 explore a set of spatial-statistical methods that provide ecologists with
19 alternative approaches for modeling spatially explicit processes that may affect
20 genetic structure. This includes an overview of spatial autoregressive models,
21 with a particular focus on how correlation and partial correlation are used to
22 represent neighborhood structure with the inverse of the covariance matrix (i.e.,
23 precision matrix). We then demonstrate how to model resistance by specifying
24 an appropriate statistical model on the nodes, conditioned on the edge weights,
25 through the precision matrix. This integration of network ecology and spatial
26 statistics provides a practical analytical framework for landscape-genetic
27 studies. The results can be used to make statistical inferences about the
28 relative importance of individual landscape characteristics, such as the
29 vegetative cover, hillslope, or the presence of roads or rivers, on gene flow. In
30 addition, the R code we include allows readers to explore landscape-genetic

31 structure in their own datasets, which will potentially provide new insights into
32 the evolutionary processes that generated ecological networks, as well as
33 valuable information about the optimal characteristics of conservation corridors.

34
35
36 KEY WORDS: spatial statistics, landscape genetics, spatially structured ecologi-
37 cal network, resistance values, edge weights

Author Manuscript

38 Introduction

39 Landscape genetics focuses on the effects of landscape pattern, structure, composition, and
40 quality on spatial-genetic variation and gene flow (Storfer et al. 2007). It is a relatively
41 new field of research (Manel et al. 2003) that draws on concepts from landscape ecology,
42 population genetics, mathematics, and statistics. However, truly integrative research is
43 challenging in this rapidly advancing field, where useful developments are occurring
44 simultaneously in multiple disciplines (Balkenhol et al. 2016a). This is especially true of
45 methods used to quantitatively describe genetic-landscape structure to gain inferences
46 about causal evolutionary and ecological processes.

47 In landscape genetics, microsatellite allele and multiple single nucleotide polymorphism
48 (SNP) data collected from individuals or populations at multiple locations are often used
49 to generate genetic distance or dissimilarity matrices, which are subsequently used to infer
50 rates of gene flow. Many different distance metrics can be used to calculate genetic
51 distances between individuals (e.g., Euclidean distance) or populations (e.g., Nei's genetic
52 distance; Nei 1972), with each relying on different geometric and/or evolutionary
53 assumptions (Dyer, 2017a). These genetic distance matrices are then used to investigate
54 how resistance to movement facilitates/prevents the dispersal of organisms and gene flow
55 (Holderegger and Wagner 2008). Within this context, landscape resistance represents the
56 effects of landscape characteristics such as vegetation or roads, on movement between them
57 (Holderegger and Wagner 2008). Evolutionary processes influencing resistance typically fall
58 into three categories: 1) isolation-by-distance (IBD), where distances between locations are

59 greater than the organisms's dispersal ability (Wright 1943); 2) isolation-by-resistance
60 (IBR), which occurs when landscape characteristics lead to inhomogeneous migration rates
61 across space (McRae 2006); and 3) isolation-by-barrier (IBB), where landscape features
62 such as waterbodies form non-permeable or semi-permeable barriers to movement (Smouse
63 et al. 1986). These relationships can be represented as a spatially structured ecological
64 network (SSEN; Dale and Fortin 2010), where nodes have a location and size, and edges
65 have a physical location and length in geographic space. Thus, the SSEN provides a
66 natural, spatially explicit framework used to explore patterns of landscape-genetic
67 structure.

68 Although inference about the relationship between resistance and genetic structure is the
69 focus of many studies, it is rare for resistance values to be measured directly using
70 empirical data (Fletcher et al. 2011). When movement is measured, it is typically based on
71 detection (i.e., sightings), relocation (i.e., mark-recapture) or pathway (i.e., global
72 positioning system telemetry) data (Zeller et al. 2012). However, resistance is more often
73 based on *a priori* experimental evidence (e.g., species dispersal ability based on telemetry
74 data) or expert opinion (Beier et al. 2008; Zeller et al. 2012). A causal-modeling approach
75 is sometimes used to compare how well the hypothesized resistance values, which are based
76 on conceptual models of evolutionary processes, fit the data (Legendre and Troussellier
77 1988; Cushman et al. 2006). Resistance estimates are crucial because they define the
78 structure of the system and underpin inferences related to dispersal, population definition,
79 and gene flow. Yet, there are significant challenges associated with validating
80 landscape-connectivity values, given that independent data are often lacking and many

81 combinations of biotic and abiotic processes could produce similar connectivity values
82 (Whitlock and McCauley 1999; Dyer and Nason 2004).

83 Spatial statistical methods are specifically designed to model spatially dependent data and
84 may be particularly suited to landscape-genetic studies. In the field of statistics, a spatial
85 statistical model uses the spatial location of data in the probabilistic model component
86 (i.e., spatial dependence in the residual errors is modeled as a function of space). These
87 models are sometimes referred to as “spatial error” models in ecology (Keitt et al. 2002).
88 Spatial autoregressive (SA) models (Lichstein et al. 2002; Ver Hoef et al. 2018) represent a
89 broad class of spatial statistical models implemented as an SSEN. Hence, there are obvious
90 conceptual similarities between landscape genetics and SA models. In landscape genetics,
91 connectivity among individuals or populations can be represented using non-binary weights
92 (i.e., resistance distance or cost-weighted distance) that may or may not incorporate a
93 physical distance; while in SA models, relationships among measurements are represented
94 in the precision matrix, which is often modeled as a function of Euclidean distance (i.e.,
95 relative weight) between locations.

96 Our goal is to describe how a spatial statistical approach can be used to model resistance in
97 landscape-genetic studies. Specifically, we 1) provide an overview of landscape-genetic data
98 and their representation as SSENs, 2) provide a brief summary of methods currently used
99 to validate models of resistance, including a synthesis of their strengths and weaknesses,
100 and 3) demonstrate how resistance distances can be estimated using SA models.

101 Modeling Spatially Structured Ecological Networks

102 CALCULATING EDGE WEIGHTS

103 A SSEN can be used to represent landscape-genetic relationships, where nodes represent
104 the location of individuals or sub-populations, and edges describe the functional
105 relationship (e.g., animal movement or gene flow) between nodes. Thus, the resistance
106 distance between nodes may differ depending on their proximity to one another, as well as
107 the landscape characteristics and features that lie between them. Such edge weights are
108 usually estimated and then validated using genetic dissimilarity between nodes because
109 data describing an organism's movement are rarely available in sufficient quantities to
110 describe the SSEN structure (Fletcher et al. 2011).

111 Contiguous nodes share a boundary, thus there is no physical distance between them;
112 therefore, covariates (i.e., predictors) representing resistance (i.e., resistance covariates) can
113 be based on node characteristics, or the distance between node centroids (Hanks and
114 Hooten 2013), that have been selected to represent an underlying conceptual model of
115 evolutionary processes (e.g., IBD, IBR, and/or IBB; Figure 1). Resistance covariates for
116 non-contiguous nodes can also be based on node characteristics (e.g., Botta et al. 2015),
117 characteristics of the edges that join node pairs (e.g. Petkova et al. 2016), or both.
118 Regardless of which method is used, *a priori* assumptions must be made about the
119 neighborhood structure, the edge location, and/or the resistance values. These assumptions
120 affect how resistance is represented in the model and the inference that can be made
121 (Figure 1).

122 Estimating edge weights for non-contiguous nodes is more complicated than for contiguous
123 nodes because the uncertainty associated with the physical edge location in geographic
124 space increases as the distance between nodes increases (i.e., multiple potential pathways
125 exist). Two approaches are commonly used to address this issue (Figure 1): 1) an *a priori*
126 decision about edge location is made, which defines the area over which resistance
127 covariates are calculated (e.g., Rioux Paquette et al. 2014); or 2) an *a priori* decision
128 about resistance values is made and edges are delineated based on those values (e.g., Beier
129 et al. 2009; Petkova et al. 2016). Many methods are used to parameterize resistance values
130 and a full review is beyond the scope of this paper (see Spear et al. (2010) and Zeller et al.
131 (2012) for in-depth reviews). However, the commonality among these methods is that *a*
132 *priori* decisions must be made about the relative importance of individual covariates of
133 resistance and/or the physical location of the edge before the edge weights are generated
134 (Figure 1). Assigning resistance values is challenging because scientific knowledge about
135 dispersal and habitat preferences is often lacking. Habitat and dispersal data may be
136 unavailable or collected at an inappropriate spatio-temporal resolution (Zeller et al. 2012).
137 Resistance values may be assigned based on expert opinion, a literature review, and/or
138 empirical data such as species occurrence, individual animal movement, rates of interpatch
139 movement, or genetic distance (Beier et al. 2008; Minor and Urban 2008; Zeller et al.
140 2012). However, there are obvious consequences in assuming that the drivers of resistance
141 and gene flow are known (Cushman et al. 2006); if this assumption is incorrect, the
142 conclusions of the study may be misleading and subsequent management actions may not
143 have the desired outcome (Shirk et al. 2010; Spear et al. 2010).

144 COMMON MODELS

145 A number of approaches are used to analyze landscape genetic-data, but the most common
146 methods generally fall into four categories: computer simulation, matrix correlation,
147 ordination, and regression (Figure 2). These methods tend to be borrowed from other
148 disciplines (Balkenhol et al. 2016a) and, as such, often do not meet basic modeling needs
149 for landscape genetic studies (Figure 2). We are not the first to point this out; there have
150 been widespread calls from landscape-genetic researchers for more robust methods of
151 exploring relationships between genetic diversity and drivers of resistance (Storfer et al.
152 2007, Balkenhol et al. 2009; Cushman and Landguth 2010; Manel and Holderegger 2013;
153 Balkenhol et al. 2016b). Some of the most common criticisms include the 1) lack of
154 statistical power, especially for small sample sizes (Legendre and Fortin 2010); 2)
155 parameter bias and low statistical power when tests are performed on spatially dependent
156 data (Legendre and Fortin 2010; Wagner and Fortin 2013); 3) inability to assess individual
157 components of resistance (e.g., vegetation cover), rather than matrices of dissimilarity, and
158 their interactions (Storfer et al. 2007; Beier et al. 2008); and 4) need for *a priori* decisions
159 about resistance values, which constrains the parameter space (Beier et al. 2008),
160 regardless of how many resistance models are proposed (e.g., Cushman and Landguth 2010,
161 Shirk et al. 2010). Despite the widespread criticisms, these methods continue to be used to
162 gain insight into evolutionary and ecological processes because there are few alternatives in
163 this emerging field of research. At the same time, there is a critical need for 1) suitable
164 methods for model selection (Cushman and Landguth 2010; Wagner and Fortin 2013) and
165 validation (Dyer and Nason 2004; Balkenhol et al. 2009); 2) statistical methods that can be

166 used to predict when the network is not fully observed (i.e., missing data; Hanks and
167 Hooten 2013) or under future land-use or climate scenarios (McRae 2006; Storfer et al.
168 2007; Beier et al. 2008); and 3) methods that describe uncertainty in resistance parameter
169 estimates (Beier et al. 2008; Zeller et al. 2012; Hanks and Hooten 2013). Thus, clear
170 methodological gaps exist and new quantitative methods are needed to make inference
171 about the suitability of these mechanistic models of connectivity and their uncertainty, as
172 well as the underlying processes that generated the network structure.

173 Spatial Autoregressive Models

174 Spatial autocorrelation underpins numerous hypotheses in ecological studies (Legendre and
175 Fortin 2010); if genetic data do not exhibit a spatial structure, then evolutionary-process
176 hypotheses related to IBD, IBR, and IBB are irrelevant. Thus, an approach that makes use
177 of spatial autocorrelation (Figure 2), rather than attempting to avoid it, is likely to provide
178 a better understanding of landscape-genetic relationships when the data are spatially
179 dependent (Balkenhol et al. 2009).

180 SA models are spatial statistical models that have been specifically designed to model areal
181 or network data. The general form of an SA model is $\{y(\mathbf{s}_i) : \mathbf{s}_i \in D, i = 1, \dots, M\}$, where y
182 is an observed (or unobserved) random variable at node i , at location \mathbf{s}_i , that belongs to
183 the spatial domain of interest, D . For example, the random variable could represent allele
184 counts, while the domain-of-interest could be a management unit. An SA model differs
185 from other spatial statistical models (e.g., geostatistical or spatial point process models)

186 because 1) D is a fixed and finite set of nodes, rather than continuous space and 2) spatial
187 dependence is modeled as a function of network structure, rather than Euclidean distance.

188 MATRIX REPRESENTATIONS OF NETWORK STRUCTURE

189 An SSEN is defined by its graphical structure (e.g., nodes and edges connecting nodes)
190 and, in a weighted network, by the weights assigned to edges (Figure 3a). To define this
191 formally, let $\mathbf{G} \equiv (\mathbf{V}, \mathbf{W})$ be an SSEN with M nodes, $\mathbf{V} \equiv \{V_1, V_2, \dots, V_M\}$, and the edges
192 or edge weights, $\mathbf{W} \equiv \{w_{ij}\}$, between them. Note that the edge weights could potentially
193 be directed (i.e., asymmetric) to account for processes such as source-sink dynamics or
194 dispersal preferences (Dale and Fortin 2010). The edges of the SSEN can also be
195 represented as an $M \times M$ matrix (Figure 3a). The element w_{ij} in the i th row and j th
196 column of the matrix \mathbf{W} is the directed or undirected edge weight connecting nodes i and j
197 in the network. In an unweighted graph, connectivity is simply represented using a binary
198 adjacency matrix, where $w_{ij} = 1$ and $w_{ij} = 0$ imply that an edge exists or does not exist
199 between nodes i and j , respectively. By definition, edges do not connect nodes to
200 themselves in SA models and therefore diagonal elements are also defined as $w_{ii} = 0$. These
201 same rules apply in a weighted network, except that $w_{ij} > 0$ indicates that there is an edge
202 between two nodes and the strength of connectivity between node pairs is allowed to vary
203 (Figure 3a). If the SSEN is undirected, then \mathbf{W} is a symmetric matrix and $w_{ij} = w_{ji}$.

CORRELATION AND PARTIAL CORRELATION

A key component of an SSEN is the conditional dependence (i.e., structure) implied by the edges. When an edge exists between nodes, $w_{ij} > 0$, then nodes i and j are first-order neighbors and are considered connected (e.g., V_1 and V_2 , Figure 3a). If two nodes are not directly connected by an edge, $w_{ij} = 0$, a path between the nodes may still exist through intervening nodes (e.g., V_2 and V_4 , Figure 3a). Thus, observations at nodes that are not first-order neighbors are conditionally independent in the precision matrix (e.g., $\mathbf{Q}_{3,2} = 0$ in Figure 3b).

A statistical concept strongly related to the network structure defined by edges is *partial correlation*. Consider the situation where a process such as genetic variation in individuals or populations, \mathbf{y} , is measured on nodes. The topological structure implied by the edges helps define the correlation structure on the process \mathbf{y} . This correlation structure is represented by $\mathbf{\Sigma}$, which is the $M \times M$ covariance matrix of \mathbf{y} (Figure 3c). Thus, the i, j th element of $\mathbf{\Sigma}$ is the covariance between y_i and y_j :

$$\Sigma_{ij} = \text{cov}(y_i, y_j) = E[(y_i - E(y_i))(y_j - E(y_j))].$$

The inverse covariance matrix, or precision matrix, $\mathbf{Q} = \mathbf{\Sigma}^{-1}$, defines the partial correlation of \mathbf{y} after accounting for the influence of intervening nodes (Figure 3b). For example, let $\{y_1, y_2, \dots, y_n\}$ be Gaussian observations on an M -node network. The partial correlation between y_i and y_j is defined as $\kappa_{ij\cdot} = \text{corr}(\varepsilon_{i\cdot}, \varepsilon_{j\cdot})$, where $\varepsilon_{i\cdot}$ are the residuals from a regression with the response y_i and $\{y_k, k \neq i, j\}$ as covariates (e.g., node size or habitat

223 quality)(Figure 3d). If $\kappa_{ij|} = 0$, then nodes i and j are not first-order neighbors and any
224 dependence between y_i and y_j is captured by intervening nodes $\{y_k, k \neq i, j\}$. For any
225 precision matrix, $\mathbf{Q}_{ij} = 0$ if and only if $\kappa_{ij|} = 0$. Thus, information about local
226 connectivity and dependence can be encoded in the precision matrix of a multivariate
227 random variable. Note that two nodes may still be correlated through intervening nodes
228 and this dependence is captured by the covariance matrix, $\mathbf{\Sigma} = \mathbf{Q}^{-1}$ ($\Sigma_{3,2} = 0.42$, Figure
229 3c), which is obtained by inverting \mathbf{Q} . This idea is conceptually similar to the role of
230 stepping stones, which promote connectivity and facilitate organism movement or gene flow
231 between isolated habitat patches (Saura et al. 2014).

232 Partial correlation is not a new concept in ecology; the partial-correlation structure
233 accommodated by the precision matrix is increasingly being used to estimate network
234 topology, which are subsequently used to understand the influence of network structure on
235 evolutionary processes (i.e., Population Graphs; Dyer and Nason 2004). However, partial
236 correlation and conditional independence in a SSEN can also be modeled as elements of the
237 precision matrix in a SA model. In the next section, we provide background information
238 about SA models for estimating edge weights using a data-driven approach.

239 CAR and ICAR Models

240 If the SA model has a Gaussian error distribution, it can be written as

$$\mathbf{y} = \mathbf{X}\boldsymbol{\alpha} + \boldsymbol{\eta} + \boldsymbol{\varepsilon}, \quad (1)$$

241 where the “error” models are $\boldsymbol{\varepsilon} \sim N(\mathbf{0}, \sigma_{\varepsilon}^2 \mathbf{I})$ and $\boldsymbol{\eta} \sim N(\mathbf{0}, \boldsymbol{\Sigma})$. The mean structure
242 describes the conditional mean of the response given a set of covariates, if they are present.
243 In Eq. 1, the mean (or first moment) structure is modeled using a regression that includes
244 covariates, \mathbf{X} , as well as a latent spatial-random process, $\boldsymbol{\eta}$. The covariates are used to
245 account for influential processes or conditions that have been measured, while the latent
246 spatial-random process is used to describe residual spatial dependence. Thus, spatial
247 dependence may result from a lack of understanding about the ecological process, an
248 inability to measure influential covariates, or inherent spatial dependence in the response
249 variable (Keitt et al. 2002). The term $\boldsymbol{\eta}$ is not directly measured and instead must be
250 inferred using a statistical model.

251 This model formulation is fundamentally different from most models built to explore
252 associations between allele prevalence and landscape features (selection), where there is
253 often no mean structure, because typical data come from neutral regions of the genome. In
254 contrast, it might be important to include covariates in the model mean structure in a
255 landscape genomics study, where allele frequencies from non-neutral regions are affected by
256 natural selection. In addition, spatial autocorrelation is not a nuisance in landscape-genetic
257 studies, but rather the main focus of the analysis. Thus, we often assume that
258 $\mathbf{y} = \boldsymbol{\eta} \sim N(\mathbf{0}, \boldsymbol{\Sigma})$. We will later consider other data models more appropriate for
259 non-Gaussian genetic data, but the Gaussian model serves as a canonical model for spatial
260 dependence in SSENs.

261 The precision matrix, $\mathbf{Q} \equiv \boldsymbol{\Sigma}^{-1}$, is used to describe the spatial dependence in the residual

262 errors and, in the case of the conditional autoregressive (CAR) model, we assume:

$$\mathbf{Q} = \mathbf{D} - \rho\mathbf{W}. \quad (2)$$

263 Here, \mathbf{W} is a binary or non-binary edge weights matrix, \mathbf{D} is a diagonal matrix with
 264 elements $D_{ii} = \sum_k W_{ik}$, and $\rho \in (0, 1)$ is a parameter affecting correlation. Other equivalent
 265 forms for the CAR precision matrix have been used in the literature (e.g.,
 266 $\mathbf{Q} = \tau^2\mathbf{M}^{-1}(\mathbf{I} - \mathbf{C})$ for matrices \mathbf{M} and \mathbf{C} ; Banerjee et al. 2004). However, the formulation
 267 in Eq. 2 highlights the direct link between the edge weights in an SSEN and the precision
 268 matrix of a spatial CAR model (Figures 3a,b).

269 The term “conditional” in the conditional autoregressive (CAR) model is used because each
 270 element of the random process is specified as conditional on those found on all first-order
 271 neighboring nodes, rather than all of the nodes (Figure 3):

$$\eta_i | \boldsymbol{\eta}_{j|j \neq i} \sim \text{N} \left(\sum_j \frac{\rho W_{ij} \eta_j}{\sum_{j \neq i} W_{ij}}, \frac{\sigma^2}{\sum_{j \neq i} W_{ij}} \right). \quad (3)$$

272 This conditional representation shows that the conditional mean of η_i is a weighted average
 273 of its neighbors ($\eta_j : j \in N(i)$, where $N(i)$ is the set of first-order neighbors of node i),
 274 scaled by ρ . If $\rho = 0$, then each η_i is independent of all other η_i , and there is no spatial
 275 autocorrelation, while larger values of ρ yield stronger correlation. If $W_{ij} > W_{ik}$, then the
 276 mean of η_i is more strongly influenced by η_j than by η_k . Thus, proportionally larger edge
 277 weights imply that there is a stronger functional relationship between nodes. Finally, the

278 conditional variance of η_i is the conditional variance parameter, σ^2 , over the sum of the
279 edge weights connected to node i . Thus, the mean and variance of the spatial random
280 process are both nonstationary, varying with node i . The conditional representation also
281 makes it clear how to model spatial correlation in SSENs using edge weights and CAR
282 models; increasing all edge weights decreases the marginal variance, while proportionally
283 larger edge weights imply stronger connectivity and correlation between nodes.

284 Correlation (Figure 3e) is a scaled version of covariance, which also contains information
285 about connectivity and dependence within the SSEN. However, the covariance and
286 correlation implied by a CAR model are sometimes counter-intuitive (Wall 2004). For
287 example, in Figure 3c, the highest covariance is found between V_1 and V_2 , but Figure 3e
288 shows that the highest correlation is found between V_1 and V_4 . This discrepancy is due to
289 the nonstationary nature of the model; in a CAR model, the least connected nodes have
290 high conditional variances (Eq. 3), and often have high marginal variances, which inflates
291 the covariance. Nevertheless, a CAR model provides some intuition on the correlation and
292 covariance implied by a SSEN. In this case, V_2 is the least connected of all nodes in the
293 network (Figure 3a), and thus it makes sense that the correlation with other nodes would
294 be relatively small.

295 An intrinsic conditional autoregressive model (ICAR; Besag and Kooperberg, 1995) is a
296 limiting case of a CAR model, where $\rho = 1$. In this case, $\mathbf{Q} = (\mathbf{D} - \mathbf{W})$ is not invertible,
297 but the ICAR can still be used as a prior in a Bayesian spatial model (e.g., Cressie 2015).
298 The covariance matrix of the ICAR can also be defined as the generalized inverse, \mathbf{Q}^- ,
299 under the constraint that the spatial-random effects sum to a constant (e.g., $\sum_{i=1}^n \eta_i = 0$)

300 (Rue and Held, 2005).

301 MISSING DATA

302 In previous sections, we assumed that all nodes in the network were fully observed and that
303 one observation, y_i , was obtained for each node, but this is unusual in practice. Consider
304 the general case where there are n_{obs} total observations at m_{nodes} nodes. When multiple
305 observations are collected on nodes (e.g., multiple individuals are genetically sampled
306 within a population), a nugget effect, τ , can be introduced into the covariance structure
307 (Besag et al. 1991) to account for within-node variation. Let $\mathbf{y} \equiv (y_1, y_2, \dots, y_{n_{obs}})'$ be the
308 vector of n_{obs} observations from the network and let Σ_{nodes} be the $m_{nodes} \times m_{nodes}$
309 covariance matrix of the entire network. When there are multiple observations on a node or
310 missing data on other nodes, there is not a one-to-one relationship between nodes and
311 observations. To account for this mismatch, an $n_{obs} \times m_{nodes}$ matrix \mathbf{K} is created to “map”
312 observations to nodes; $K_{ij} = 1$ if the i th observation (y_i) is taken at the j th node, and
313 $K_{ij} = 0$ otherwise. The matrix \mathbf{K} can then be used in the $n_{obs} \times n_{obs}$ covariance matrix Ψ
314 of the observations \mathbf{y} , where

$$\Psi = \mathbf{K}\Sigma\mathbf{K}' + \tau^2\mathbf{I}.$$

315 Estimation of the edge weights, which define Σ , can then be carried out by substituting Ψ
316 for Σ in a CAR or ICAR model.

317 The ability to use the entire network in the modeling process has numerous advantages,
318 even if it is partially unobserved. Nodes with missing data are usually removed from the

319 analysis, which equates to a loss of information (Nakagawa and Freckleton 2008). If data
320 are not missing at random, it alters the topology of the network (Kossinets 2006; Fletcher
321 et al. 2011), results in loss of statistical power, and produces biased parameter estimates
322 for processes on the network (Nakagawa and Freckleton 2008). A covariance matrix that
323 represents all of the network nodes can also be used within a SA model to make
324 predictions, with estimates of uncertainty, at unobserved nodes. These predictions provide
325 estimates of processes on, and the topology of a network that has not been fully observed
326 based on the observed data. However, they can also be used for model validation in a
327 k-fold cross-validation procedure. Another important advantage is the ability to
328 incorporate nodes with missing data into the statistical model, which means that a
329 contiguous data model can be used to estimate resistance; thus, removing the need to make
330 *a priori* and potentially incorrect assumptions about the spatial location of edges between
331 non-contiguous nodes (Figure 1). Although there may not be a partial correlation between
332 two observed nodes separated by nodes with missing values, spatial dependence may still
333 exist because of the intervening nodes in the path between them (Figure 3c).

334 Edge Weight Estimation Using Spatial Autoregressive 335 Models

336 Although SA models are often used in spatial statistics, the specification of weights has
337 received little attention. In most cases, weights are arbitrarily described using
338 representations of adjacency with little thought devoted to the processes that drive

339 connectivity. When weights are specified in this manner, they are considered fixed and
340 known, which implies that the topology of the SSEN is known exactly; however, this is
341 almost never the case in ecology. In fact, ecological questions often *focus* on understanding
342 the drivers of landscape connectivity. We reconcile these statistical and ecological
343 perspectives, with the goal of gaining a better ecological understanding of resistance in
344 SSENs.

345 Characteristics on the nodes (e.g., habitat quality, size, or population size) or along the
346 edges (e.g., length, vegetation cover, or barriers to movement) may describe
347 increases/decreases in landscape connectivity between node pairs. Thus, the resistance
348 distance between nodes may, or may not, be solely dependent on the physical distance
349 between them. Here we define resistance distance as the cumulative resistance between
350 observations based on circuit theory (McRae 2006, Zeller et al. 2012). For example, if the
351 nodes are irregularly spaced or irregular in size, it would make sense to model connectivity
352 (i.e., edge weights) as a function of distance between nodes. The most natural approach is
353 to treat the centroid of each node as the location, and include the distance, or log-distance
354 (Hanks and Hooten 2013) between nodes as a resistance covariate in Eq. (5), with or
355 without other resistance covariates.

356 An SA model may include a multivariate response, y_i , such as microsatellites or multiple
357 SNPs for individuals or populations. The CAR or ICAR model can be connected to more
358 ecologically relevant network-based approaches when the weights matrix is constructed.
359 Instead of defining edge weights based on conceptual models of evolutionary processes,
360 Hanks and Hooten (2013) showed that they may be estimated by specifying an appropriate

361 statistical model for \mathbf{y} , conditioned on the edge weights through the precision matrix. For
362 example, edge weights, w_{ij} , could be modeled as

$$w_{ij} = \begin{cases} 0 & \text{if } i \text{ and } j \text{ are not first-order neighbors,} \\ f(\mathbf{x}_{ij}, \boldsymbol{\beta}) & \text{if } i \text{ and } j \text{ are first-order neighbors,} \end{cases} \quad (4)$$

363 where \mathbf{x}_{ij} is a vector of covariates used to model the edge weight between i and j (e.g., slope
364 or vegetation cover), and $\boldsymbol{\beta}$ is a vector of estimated parameters. Edge weights are usually
365 greater than zero, thus one potential model relating \mathbf{x}_{ij} and w_{ij} is a log-linear model:

$$f(\mathbf{x}_{ij}, \boldsymbol{\beta}) = \exp\{\mathbf{x}'_{ij}\boldsymbol{\beta}\}. \quad (5)$$

366 For the IBD model, $f(\mathbf{x}_{ij}, \boldsymbol{\beta}) \equiv 1$ so we obtain an estimated distance-only decay function,
367 with no other effects, that depends conditionally on first-order neighbors; although
368 autocorrelation decays with distance throughout the study area (e.g., Ver Hoef et al. 2018).
369 Many other model formulations are also possible. For example, in Ver Hoef et al. (2018), $\boldsymbol{\beta}$
370 was estimated as a function of categorical variables representing differences in harbor seal
371 sub-population membership. Similarly, the matrix \mathbf{x}_{ij} could contain extra resistance
372 covariates for models representing the IBR (e.g., vegetation cover) and IBB (e.g., rivers)
373 evolutionary-process hypotheses, in addition to an intercept.

374 As mentioned previously, models are often fit to genetic distance or diversity matrices in
375 landscape-genetic studies and these matrices can be generated based on a variety of
376 distance metrics. For example, Wright's F_{ST} (Wright 1931) and Nei's D (Nei 1972) can be

377 used to describe population-based genetic diversity, while the Bray-Curtis (Legendre and
378 Legendre 2012) and other measures of relatedness (Queller and Goodnight 1989) are
379 typically used to measure individual-level genetic diversity. However, the advantages of
380 modeling genetic distance using an SA model as described here are only realized if there is
381 an appropriate statistical distribution for an observed distance matrix and the covariance
382 matrix. The generalised Wishart distribution has been used in recent landscape-genetic
383 studies to visualise patterns of population structure (Bradburd et al. 2016) and to estimate
384 ancestry proportions from multiple populations (Bradburd et al. 2018). McCullagh (2009)
385 showed that a generalized Wishart distribution is the appropriate statistical model if the
386 genetic distance matrix, \mathbf{D} , is based on squared-Euclidean distance of a normally
387 distributed random variable (Appendix S1). Under these assumptions, $-\mathbf{D} \sim \text{GW}_\nu(\mathbf{1}, \mathbf{2}\Sigma)$,
388 where $\Sigma = \mathbf{Q}^{-1}$. However, there is no guarantee that the generalized Wishart distribution
389 will be appropriate for all dissimilarity matrices and future research is needed to develop
390 diagnostic tools to check the validity of these distributional assumptions. The advantage of
391 this approach is that it provides a formal statistical likelihood for pairwise distance data.
392 This makes the whole range of likelihood-based tools such as maximum likelihood
393 estimation, asymptotic confidence intervals on parameters, and model selection using
394 Akaike's information criterion (AIC; Akaike 1974) and other information criteria applicable
395 to genetic analyses. Another major benefit is that the parameter estimates, β (Eq. 5), are
396 comparable between different populations and studies. As a result, it is possible to fit
397 similar models to multiple disparate populations and assess how consistent the
398 landscape-genetic relationships are.

399 Under a CAR model, the edge weights \mathbf{W} and the parameter ρ completely define \mathbf{Q} and Σ
400 (Figures 3b,c), and the likelihood of the data under the generalized Wishart model.
401 Multiple conceptual models of connectivity could be specified using different formulations
402 of \mathbf{W} or Σ and compared using AIC. This provides a flexible modeling framework, where
403 genetic data on the nodes are converted to genetic data on the edges (e.g., genetic-distance
404 matrices), and modeled as a function of covariates on the nodes (e.g., node or
405 neighborhood level) and/or edges of the SSEN. This method does not fit neatly into the
406 four levels of analysis proposed by Wagner and Fortin (2013) to relate genetic data to
407 landscape data (e.g., node, link, neighborhood, and boundary). Instead, we refer to it as a
408 *network-based* method because it can be used to represent all four levels of analysis,
409 depending on how the model is parameterized and the research question of interest.

410 SIMULATED EXAMPLE

411 Observed genetic patterns may be produced by the combined influence of geographic
412 distance, resistance, and barriers, rather than a single evolutionary process (Landguth and
413 Cushman 2010). The SA model can be used to account for proximity in terms of variables
414 on nodes and/or edges, physical distance (e.g., Euclidean or least-cost path), and
415 unobserved drivers of landscape connectivity. Next, we provide an example demonstrating
416 how edge weights can be estimated within an ICAR model by incorporating resistance
417 covariates into the off-diagonal elements of the precision matrix. We provide data (dataS1
418 and dataS2) and R code (dataS1 and Appendix S2) so that readers can recreate the
419 example.

420 We simulated resistance surfaces for the IBD, IBR, and the IBB scenarios (Figure 4,
 421 Appendix S2). The locations for 30 subpopulations were randomly generated and the
 422 pairwise resistance distance was calculated based on the IBD, IBR, and IBB models
 423 (Appendix S2). This distance is equivalent to the cumulative resistance between
 424 population locations based on circuit theory (McRae et al. 2008).

425 Genetic data were simulated under the IBD, IBR, and IBB evolutionary-process models for
 426 450 individuals (30 subpopulations x 15 individuals) using the PopGenReport package
 427 (Adamack and Gruber 2014, Appendix S2). Genetic distance matrices for individual allele
 428 counts were calculated for the simulated datasets based on Manhattan distance.

429 We fit three models (IBD, IBR, and IBB) to each of the genetic-distance matrices (\mathbf{D}_{IBD} ,
 430 \mathbf{D}_{IBR} , \mathbf{D}_{IBB}) using a generalized Wishart distribution (Appendix S1). The nine models had
 431 the form

$$-\mathbf{D} \sim \text{GW}_{\nu}(\mathbf{1}, \mathbf{2}\Psi), \quad (6)$$

432 where GW is the generalised Wishart distribution and $\nu = 20$ represents the number of
 433 genetic loci used to compute \mathbf{D} .

434 The SA models were fit using a raster-based network representation, with contiguous nodes
 435 and edge weights (and corresponding off-diagonal elements of the ICAR precision matrix) a
 436 function of the distance between node centroids, and the resistance value at neighboring
 437 raster cells estimated from the data. The spatial covariance for the models was given by

$$\Psi = \mathbf{KQ}^{-1}\mathbf{K}' + \tau^2\mathbf{I}, \quad (7)$$

438 where \mathbf{K} is a design matrix linking observations to nodes (raster cells) in the SSEN, τ^2
439 models non-spatial variability, and \mathbf{Q} is an ICAR precision matrix (Eq. 2), with edge
440 weights a function of resistance covariates, \mathbf{x}_{ij} , as shown in Figure 4.

441 The edge weights were modeled as a log-linear function of an intercept only for the IBD
442 model, an intercept and a continuous resistance covariate for the IBR model, and an
443 intercept and a binary covariate representing a non-permeable barrier to movement for the
444 IBB model (Figure 4). Notice that the IBR and IBB models account for both resistance
445 covariates *and* the distance between individuals, while the IBD model is based purely on
446 distance. Parameters were estimated using maximum likelihood.

447 We compared the models using AIC (Akaike 1974) and found that for \mathbf{D}_{IBD} , the data
448 generating model (IBD) had slightly more support in the data than the IBR estimating
449 model, and considerably more support than IBB (Table 1). This is not surprising based on
450 the patterns observed in the simulated genetic distance versus resistance plots (Appendix
451 S2). However, there was no question about which models had the most support in the data
452 for \mathbf{D}_{IBR} and \mathbf{D}_{IBB} . The AIC value for the IBR data-generating model was more than 14
453 units lower than the competing IBD and IBB estimating models for \mathbf{D}_{IBR} , while the AIC
454 for the \mathbf{D}_{IBB} data-generating model (IBB) was more than 56 units lower than alternative
455 IBD and IBR estimating models (Table 1).

456 The exponentiated β parameter estimates produced by the final models describe the
457 relationship between the conductance (i.e., 1/resistance) and the original resistance
458 covariates (Figure 4) and this relationship can be plotted, with 95% confidence intervals.
459 Figure 5a shows that the relationship between conductance and the resistance covariate

460 described by the fitted \mathbf{D}_{IBR} data-generating model is non-linear, which is not surprising
461 given that a log-linear model was used. As expected, conductance through cells with low
462 IBR resistance-covariate values is higher than those with larger values, with conductance
463 dropping off rapidly as resistance increases from 1 to 5. The 95% confidence intervals show
464 that there is more uncertainty about this relationship when resistance is moderate (e.g., 5
465 to 10) compared to when it is low or high (Figure 5a). The relatively low AIC value for
466 this model (Table 1) indicates that the \mathbf{D}_{IBR} data-generating model was able to describe
467 this relationship more accurately than the other models and thus provides greater insight
468 into the relationship between the IBR resistance covariate and simulated gene flow.
469 Furthermore, maps of conductance generated using the SA model (Figure 5b) could be
470 used to define movement corridors between conservation reserves or examine scenarios of
471 land-management impacts on gene flow (e.g., McRae et al. 2008; Landguth and Cushman
472 2010).

473 Considerations

474 The benefit of using SA models with SSENs is the ability to model spatially dependent data
475 and gain statistically robust inferences. However, the advantages gained in fitting a SA
476 model strongly depend on the genetic distance matrices containing sufficient information to
477 estimate edge weights. In other words, there must be relatively strong spatial dependence
478 in the data and this is affected by both the genetic and field survey design.

479 Genetic data are collected from individuals at multiple locations in landscape-genetic

480 studies, and often transformed into a genetic distance matrix prior to modelling. These
481 matrices are usually based on a subset of alleles found on neutral loci (i.e., microsatellite
482 alleles or SNPs) that have no known function and as such, are not believed to be involved
483 in natural selection (Wagner and Fortin 2013). Instead, the variability in the genetic data
484 should reflect genetic drift; highlighting the influence of landscape resistance on gene flow
485 and population structure. There are numerous filtering steps designed to reduce the
486 negative effects of sequencing errors, missing data, duplicated loci, linkage disequilibrium,
487 deviations from Hardy-Weinberg equilibrium, and polymorphism (Benestan et al. 2016).
488 As noted by the authors, these choices can affect inferences in models fit to genetic data,
489 but filtering decisions will be dependent on the dataset and the research question of interest
490 (Andrews et al. 2016). The initial choice of alleles was particularly important in the past,
491 when it was often cost prohibitive to sample more than 20 loci (Waits and Storfer 2016).
492 However, with the advent of next generation sequencing, it is not uncommon to obtain
493 genetic data at tens of thousands of loci. As a result, genetic sampling is expected to be
494 the least limiting factor in future landscape-genetic studies (Balkenhol and Fortin 2016).
495 The field survey design is another important consideration, but the optimal design is
496 expected to differ depending on the environment and species-of-interest (Balkenhol and
497 Fortin 2016). The number of individuals must be sufficient to represent the genetic
498 diversity in the population and appropriate for the research question (Waits and Storfer
499 2016). If the genetic diversity is low, then it may be captured with a relatively small
500 number of individuals and alleles; while more individuals and alleles will be required when
501 genetic diversity is high. In rare cases, power analysis is used to identify the minimum

502 sample size needed (Ryman and Palm 2006). Simulation studies can also help identify the
503 minimum number of individuals and sub-populations needed to detect the effects of
504 distance and landscape resistance on gene flow (Manel et al. 2012). General rules of thumb
505 have been proposed, suggesting that 20 to 30 individuals are needed when using
506 microsatellite data (Hale et al. 2012). However, these numbers are insufficient for the SA
507 models described here. Instead, larger minimum sample sizes are needed (>100
508 observations in our experience) due to the additional parameters being estimated and the
509 loss of effective degrees of freedom. Larger sample sizes may also be needed as the
510 complexity of the edge-weights model increases. Nevertheless, sample size may not be an
511 issue in many studies, where researchers have artificially decreased the sample size by
512 aggregating genetic data from individuals to the sub-population level. Aggregation is not
513 necessary using this approach, which implies that researchers can make use of all of their
514 genetic data. Although estimating the edge weights within a SA modeling framework may
515 not be possible for every existing dataset, future studies could be designed to meet these
516 requirements.

517 Finally, it is important to keep in mind that correlation does not equal causation. Many
518 different environmental and biological processes can affect genetic dissimilarity between
519 individuals and populations, and it is possible that patterns in resistance covariates and
520 distance measures mimic patterns produce by the true causal factor (Rellstab et al. 2015).
521 For example, if alleles are incorrectly assumed to be neutral, selection may be causing a
522 particular pattern in genetic differentiation rather than resistance to gene flow (Whitlock
523 and McCauley 1999). Alternatively, migration and drift may not have reached equilibrium

524 for populations that are currently expanding and as a result, patterns in genetic
525 differentiation would not necessarily reflect current patterns in gene flow (Whitlock and
526 McCauley 1999). Even when assumptions such as these are correct, multiple landscape
527 genetic hypotheses are often highly correlated (Murphy et al. 2008); as was the case here,
528 where we observed similar correlations between genetic data generated using an IBD model
529 (D_{IBD}) and an IBR estimating model (Appendix S2). Thus, it is important that *a priori*
530 hypotheses describing the effects of landscape resistance on gene flow are carefully
531 constructed based on current scientific knowledge, and tested using sophisticated and
532 robust modelling approaches (Cushman and Landguth 2010), such as those described here.

533 Conclusions

534 There is an undeniable need for quantitative methods in landscape genetics that can be
535 used to explore questions about spatial structure in genetic datasets. SA models provide a
536 natural framework to investigate those questions. Spatial autocorrelation underpins
537 common evolutionary-process hypotheses in landscape-genetic studies and thus it is
538 sensible to use a statistical method that incorporates spatial autocorrelation (Balkenhol et
539 al. 2009). SA models are designed to describe the neighborhood structure in spatially
540 correlated network data and provide a flexible probabilistic framework used to make
541 inferences about the effects of habitat selection and movement preferences on gene flow.
542 The data model for these *network-level* analyses may include raw genetic data or genetic
543 distance matrices, as well as covariates on nodes and edges. Covariates representing

544 multiple evolutionary-process hypotheses can also be assessed within a single modeling
545 framework, which produces interpretable parameter estimates for resistance components,
546 with uncertainty estimates, so that inferences can be made about their relative influence
547 within and between populations. In addition, standard model selection methods, such as
548 regularization or information-theoretic-based approaches, may be used to compare and
549 select among models (Hooten and Hobbs 2015); while predictions, with estimates of
550 uncertainty, can be made at unobserved locations or under different land-use or climate
551 scenarios. The ability to predict provides management benefits (Storfer et al. 2007), but
552 can also be used to validate models using k-fold cross-validation. Most notably, the ability
553 to account for missing data within the SA model means that a contiguous data model can
554 be used when resistance values are estimated. Thus, *a priori* assumptions about the spatial
555 location of edges between non-contiguous nodes, the relative influence of individual
556 resistance covariates, and the overall resistance between nodes are avoided. Closer
557 collaboration between ecologists and spatial statisticians will lead to new methods that are
558 specifically designed to answer spatial and spatio-temporal questions about connectivity in
559 landscape-genetic studies.

560 **Acknowledgments**

561 We would like to thank two anonymous reviewers and Dr Paul Conn for the constructive
562 comments and suggestions they provided on a previous version of this manuscript. This
563 research began from a network-model working group at the Statistics and Applied

564 Mathematical Sciences (SAMSI) 2014-15 Program on Mathematical and Statistical
565 Ecology. The National Science Foundation, Division of Mathematical Sciences,
566 collaborative research project 1614392 also provided support for this research. Any use of
567 trade, firm, or product names is for descriptive purposes only and does not imply
568 endorsement by the U.S. Government.

569 **References**

- 570 Adamack, A.T., & Gruber, B. (2014) PopGenReport: simplifying basic population genetic
571 analyses in R. *Methods in Ecology and Evolution*, 5(4), 384–387.
- 572 Akaike, H. 1974. A new look at the statistical model identification, *IEEE Transactions on*
573 *Automatic Control*, 19(6): 716–723.
- 574 Andrews K.R., Good, J.M., Miller, M.R., Luikart, G., Hohenlohe, P.A. (2016) Harnessing
575 the power of RADseq for ecological and evolutionary genomics. *Nature Reviews Genetics*,
576 17: 81–92.
- 577 Balkenhol, N., Waits, L.P. & Dezzani, R.J. (2009) Statistical approaches in landscape
578 genetics: An evaluation of methods for linking landscape and genetic data. *Ecography*, 32:
579 818–830.
- 580 Balkenhol, N., Cushman, S.A., Storfer, A. & Waits, L.P. (2016a) Introduction to landscape
581 genetics: Concepts, methods, and applications, Chapter 1 *In: Landscape Genetics:*
582 *Concepts, Methods, and Applications.* (eds.) Balkenhol N., Cushman S.A., Storfer A.T., &

583 Waits L.P., John Wiley & Sons, Hoboken, NJ. pg. 247–255.

584 Balkenhol, N., Cushman, S.A., Storfer, A. & Waits, L.P. (2016b) Opportunities, and
585 remaining challenges in landscape genetics, Chapter 14 *In: Landscape Genetics: Concepts,*
586 *Methods, and Applications.* (eds.) Balkenhol N., Cushman S.A., Storfer A.T., & Waits
587 L.P., John Wiley & Sons, Hoboken, NJ. pg. 1–7.

588 Balkenhol, N., & Fortin M.–J. (2016) Basics of study design: Sampling landscape
589 heterogeneity and genetic variation for landscape genetic studies. Chapter 4 *In: Landscape*
590 *Genetics: Concepts, Methods, Applications, First Edition.* Eds: Balkenhol, N., Cushman,
591 S.A., Storfer, A.T., and Waits, L.P. John Wiley & Sons, Ltd. 58–76.

592 Banerjee, S., Carlin, B.P. & Gelfand, A.E. 2004. Hierarchical modeling and analysis for
593 spatial data. Boca Raton, FL, USA: Chapman & Hall/CRC.

594 Beier, P., Majka, D.R. & Spencer W.D. (2008) Forks in the road: Choices in procedures for
595 designing wildland linkages. *Conservation Biology*, 22(4): 836 to 851.

596 Beier, P., Majka, D.R., & Newell, S.L. (2009) Uncertainty analysis of least-cost modeling
597 for designing wildlife linkages. *Ecological Applications*, 19(8): 2067–2077.

598 Benestan, L.M., Ferchaud, A.–L., Hohenlohe, P.A., Garner, B.A., Naylor, G.J., Baums,
599 I.B., Schwartz, M.K., Kelley, J.L., & Luikart, G. (2016) Conservation genomics of natural
600 and managed populations: building a conceptual and practical framework. *Molecular*
601 *Ecology*, 25: 2967–2977.

602 Besag, J., York, J. & Mollié, A. (1991) Bayesian image restoration, with two applications
603 in spatial statistics. *Annals of the Institute of Statistical Mathematics*, 43(1):1–20.

604 Besag, J. & Kooperberg, C. 1995. On conditional and intrinsic autoregressions.
605 *Biometrika*, 82(4): 733–746.

606 Botta, F., Eriksen, C., Fontaine, M.C., & Guillot, G. (2015) Enhanced computational
607 methods for quantifying the effect of geographic and environmental isolation on genetic
608 differentiation. *Methods in Ecology and Evolution*, 6: 1270–1277.

609 Bradburd, G.S., Ralph, P.L., and Coop, G.M. (2016) A spatial framework for understanding
610 population structure and admixture. *PLoS Genetics*, 12(1): e1005703.
611 doi:10.1371/journal.pgen.1005703.

612 Bradburd, G.S., Coop, G.M., & Ralph, P.L. (2018) Inferring continuous and discrete
613 population genetic structure across space. *Genetics*, 210: 33–52.

614 Cressie, N. (2015) *Statistics for Spatial Data*, Revised Edition. John Wiley & Sons, Inc.,
615 Hoboken, USA. 928p.

616 Cushman, S.A. & Landguth, E.L. (2010) Spurious correlations and inference in landscape
617 genetics. *Molecular Ecology*, 19: 3592–3602.

618 Cushman, S.A., McKelvey, K.S., Hayden, J. & Schwartz, M.K. (2006) Gene flow in
619 complex landscapes: Testing multiple hypotheses with causal modeling. *The American*
620 *Naturalist*, 168(4): 486–499.

621 Dale, M.R.T. & Fortin, M.-J. (2010) From graphs to spatial graphs. *Annual Review of*
622 *Ecology, Evolution, and Systems*, 41, 21–38.

623 Dyer, R.J. & Nason, J.D. (2004) Population graphs: the graph-theoretic shape of genetic

624 structure. *Molecular Ecology*, 13, 1713–1728.

625 Dyer, R.J. (2017) Genetic Distances, In: *Applied Population Genetics*, Chapter 20.

626 Retrieved on October 10, 2018 from:

627 https://dyerlab.github.io/applied_population_genetics/genetic-distances.html

628 Epperson, B.K., McRae, B.H., Scribner, K., Cushman, S.A., Rosenberg, M.S., Fortin,
629 M.-J., James, P.M.A., Murphy, M., Manel, S., Legendre, P., & Dale, M.R.T. (2010) Utility
630 of computer simulations in landscape genetics. *Molecular Ecology*, 19, 3549–3564.

631 Fletcher, R.J., Acevedo, M.A., Reichert, B.E., Pias, K.E. & Kitchens, W.M. (2011) Social
632 network models predict movement and connectivity in ecological landscapes. *Proceedings*
633 *of the National Academy of Sciences*, 108(48): 19282–19287.

634 Fotheringham, A.S. & O’Kelly, M.E. (1989) *Spatial interaction models: Formulation and*
635 *applications*. Kluwer Academic Publishers, Dordrecht.

636 Fortin, M.-J. & Dale, M.R.T. (2014) *Spatial Analysis: A guide for ecologists*. Second
637 Edition. Cambridge University Press, Cambridge, UK. 438p.

638 Hale, M.L., Burg, T.M., & Steeves, T.E. (2012) Sampling for microsatellite-based
639 population genetic studies: 25 to 30 individuals per population is enough to accurately
640 estimate allele frequencies. *PloS One* 7, e45170.

641 Hanks, E.M. & Hooten, M.B. (2013) Circuit theory and model-based inference for
642 landscape connectivity. *Journal of the American Statistical Association*, 108(501): 22–33.

643 Hanks, E.M. (2017) *rwc: Random Walk Covariance Models*. R package verion 1.1,

644 <https://CRAN.R-project.org/package=rwc>.

645 Holderegger, R. & Wagner, H.H. (2008) Landscape Genetics. *Bioscience*, 58(3): 199–207.

646 Hooten, M.B. & Hobbs, N.T. (2015) A guide to Bayesian model selection for ecologists.
647 *Ecological Monographs*, 85(1): 3–28.

648 Jombart, T., Devillard, S., Dufour, A.-B. & Pontier, D. (2008) Revealing cryptic spatial
649 patterns in genetic variability by a new multivariate method. *Heredity*, 101: 92–103.

650 Jombart, T., Pontier, D. & Dufour, A.-B. (2009) Genetic markers in the playground of
651 multivariate analysis. *Heredity*, 102: 330–341.

652 Keitt, T.H., Bjornstad, O.N., Dixon, P.M. & Citron-Pousty, S. (2002) Accounting for
653 spatial pattern when modeling organism-environment interactions. *Ecography*, 25(5):
654 616–625.

655 Kossinets, G. (2006) Effects of missing data in social networks. *Social Networks*, 28:
656 247–268.

657 Landguth, E.L. & Cushman, S.A. (2010) CDPOP: A spatially explicit cost distance
658 population genetics program. *Molecular Ecology Resources*, 10: 156–161.

659 Legendre, P., Lapointe, F. & Casgrain, P. (1994) Modeling brain evolution from behavior:
660 A permutational regression approach. *Evolution*, 48: 1487–1499.

661 Legendre, P. & Fortin, M.-J. (2010) Comparison of the Mantel test and alternative
662 approaches for detecting complex multivariate relationships in the spatial analysis of
663 genetic data. *Molecular Ecology Resources*, 10: 831–844.

- 664 Legendre, P. & Legendre, L.F.J. (2012) Numerical Ecology. Developments in
665 Environmental Modelling Series, 24. Elsevier, New York, USA. 1006p.
- 666 Legendre, P. & Trousselier, M. (1988) Aquatic heterotrophic bacteria: modeling in the
667 presence of spatial autocorrelation. *Limnology and Oceanography*, 33:1055–1067.
- 668 Lichstein, J.W., Simons, T. R., Shriener, S.A., and Franzreb, K.E. 2002. Spatial
669 autocorrelation and autoregressive models in ecology. *Ecological Monographs* 72: 445–463.
- 670 Manel, S., Schwartz, M.K., Luikart, G. & Taberlet, P. (2003) Landscape genetics:
671 combining landscape ecology and population genetics. *Trends in Ecology & Evolution*,
672 18(4): 189–197.
- 673 Manel, S., Albert, C.H., & Yoccoz, N.G. (2012) Sampling in landscape genomics. In: *Data
674 Production and Analysis in Population Genomics*. Eds. Pompanon, F., Bonin, A. Human
675 Press, New York, Pages 3–12.
- 676 Manel, S. & Holderegger, R. (2013) Ten years of landscape genetics. *Trends in Ecology &
677 Evolution*, 28(10): 614–621.
- 678 Mantel, N. (1967) The detection of disease clustering and a generalized regression
679 approach. *Cancer Research*, 27: 209–220.
- 680 McCullagh, P. (2009) Marginal likelihood for distance matrices. *Statistica Sinica*, 19:
681 631–649.
- 682 McRae, B.H. (2006) Isolation by resistance. *Evolution*, 60: 1551–1561.
- 683 McRae, B.H., Dickson, B.G., Keitt, T. & Shah, V.B. (2008) Using circuit theory to model

684 connectivity in ecology, evolution, and conservation. *Ecology*, 89(10): 2712–2724.

685 Minor, E.E. & Urban, D.L. (2008) A graph-theory framework for evaluating landscape
686 connectivity and conservation planning. *Conservation Biology*, 22: 297–307.

687 Murphy, M.A., Evans, J.S., Cushman, S.A., & Storfer, A. (2008) Representing genetic
688 variation as continuous surfaces: An approach for identifying spatial dependency in
689 landscape genetic studies. *Ecography*, 31:685–697.

690 Murphy, M.A., Dezanini, R.J., Pilliod, D. & Storfer, A. (2010) Landscape genetics of high
691 mountain frog metapopulations. *Molecular Ecology*, 19: 3634–3649.

692 Murphy, M.A., Dyer, R. & Cushman, S.A. (2016) Graph theory and network models in
693 landscape genetics, Chapter 10. *In: Landscape Genetics: Concepts, Methods, and
694 Applications.* (eds.) Balkenhol N., Cushman S.A., Storfer A.T., & Waits L.P., John Wiley
695 & Sons, Hoboken, NJ. pg. 165–179.

696 Nakagawa, S. & Freckleton, R.P. (2012) Missing inaction: the dangers of ignoring missing
697 data. *Trends in Ecology and Evolution*, 23(11): 592–596.

698 Nei, M. (1972) Genetic distance between populations. *American Naturalist*, 106: 283–292.

699 Petkova, D., Novembre, J. & Stephens, M. (2016) Visualizing spatial population structure
700 with estimated effective migration surfaces. *Nature Genetics*, 48(1): 94–100.

701 Queller, D.C. & Goodnight, K.F. (1989) Estimating relatedness using genetic markers.
702 *Evolution*, 43(2): 258–275.

703 R Core Team (2016) R: A language and environment for statistical computing. R

704 Foundation for Statistical Computing. Vienna, Austria. <https://www.R-project.org>.

705 Rellstab, C., Gugerli, F., Eckert, a.J., Hancock, A.M., & Holderegger, R. (2015) A practical
706 guide to environmental association analysis in landscape genomics. *Molecular Ecology*, 24:
707 4348–4370.

708 Rioux Paquette, S.R., Talbot, B., Garant, D., Mainguy, J. & Pelletier, F. (2014) Modelling
709 the dispersal of the two main hosts of the raccoon rabies variant in heterogeneous
710 environments with landscape genetics. *Evolutionary Applications*, 7(7): 734–749.

711 Rue, H., and Held, L. (2005) *Gaussian Markov Random Fields: Theory and Applications*,
712 in *Monographs on Statistics and Applied Probability* (Vol. 104), Boca Raton, FL: Chapman
713 & Hall.

714 Ryman, N. & Palm, S. (2006) POWSIM: a computer program for assessing statistical
715 power when testing for genetic differentiation. *Molecular Ecology Notes*, 6: 600–602.

716 Saura, S., Bodin, Ö & Fortin, M.-J. (2014) Stepping stones are crucial for species'
717 long-distance dispersal and range expansion through habitat networks. *Journal of Applied*
718 *Ecology*, 51(1): 171–182.

719 Shirk, A.J., Wallin, D.O., Cushman, S.A., Rice, C.G. & Warheit, K.I. (2010) Inferring
720 landscape effects on gene flow: a new model selection framework. *Molecular Ecology*, 19:
721 3603–3619.

722 Smouse, P.E., Long, J.C. & Sokal, R.R. (1986) Multiple regression and correlation
723 extensions of the Mantel test of matrix correspondence. *Systematic Zoology*, 35, 627–632.

724 Spear, S.F., Balkenhol, N., Fortin, M.-J., McRae, B.H. & Scribner, K. (2010) Use of
725 resistance surfaces for landscape genetic studies. *Molecular Ecology*, 19: 3576–3591.

726 Storfer, A., Murphy, M.A., Evans, J.S., Goldberg, C.S., Robinson, S., Spear, S.F., Dezzani,
727 R., Delmelle, E., Vierling, L. & Waits, L.P. (2007) Putting the ‘landscape’ in landscape
728 genetics. *Heredity*, 98–142.

729 ter Braak, C.J.F. (1986) Canonical correspondence analysis: a new eigenvector technique
730 for multivariate direct gradient analysis. *Ecology*, 67(5): 1167–1179.

731 Ver Hoef, J.M, Peterson, E.E., Hooten, M.B., Hanks, E.M. & Fortin, M.-J. (2018) Spatial
732 autoregressive models for statistical inference from ecological data. *Ecological Monographs*,
733 88(1): 36–59.

734 Wagner, H.H. & Fortin, M.-J. (2013) A conceptual framework for the spatial analysis of
735 landscape genetic data. *Conservation Genetics*, 14: 253–261.

736 Waits, L.P. & Storfer, A. (2016) Basics of population genetics, Chapter 3 In: *Landscape*
737 *Genetics: Concepts, Methods, Applications*, First Edition. Eds: Balkenhol, N., Cushman,
738 S.A., Storfer, A.T., and Waits, L.P. John Wiley & Sons, Ltd. Pages 35–57.

739 Wall, M.M. (2004) A close look at the spatial structure implied by the CAR and SAR
740 models. *Journal of Statistical Planning*, 121: 311–324.

741 Whitlock, M.C. & McCauley, D.E. (1999) Indirect measures of gene flow and migration:
742 $F_{ST} \neq 1/(fNm + 1)$. *Heredity*, 82:117–125.

743 Wright, S. (1931) Evolution in Mendelian populations. *Genetics*, 16(2): 97–159.

744 Wright, S. (1943) Isolation by distance. *Genetics*, 28: 114–138.

745 Zeller, K.A., McGarigal, K. & Whiteley, A.R. (2012) Estimating landscape resistance to
746 movement: A review. *Landscape Ecology*, 27: 777–797.

747 **Data Availability**

748 Data and R code associated with this study are available on Data Dryad.

Author Manuscript

Table 1: The Akaike Information Criteria (AIC) values for the models based on simulated genetic distance (D_{IBD} , D_{IBR} , D_{IBB}) and the three resistance models: isolation by distance (IBD), isolation by resistance (IBR), and isolation by barrier (IBB).

Genetic Distance	Resistance Model	AIC
D_{IBD}	IBD	22518.94
D_{IBD}	IBR	22520.23
D_{IBD}	IBB	22527.61
D_{IBR}	IBD	22589
D_{IBR}	IBR	22573.6
D_{IBR}	IBB	22588.43
D_{IBB}	IBD	20414.75
D_{IBB}	IBR	20399.52
D_{IBB}	IBB	20342.68

750 Figure Captions

751 Figure 1. The data format of the spatially structured ecological network affects the way
752 that edge weights are generated. Resistance covariates for contiguous nodes are based on
753 node characteristics, but can be node- and/or edge-based for non-contiguous nodes.

754 Regardless of the data format, *a priori* assumptions about the neighborhood structure,
755 edge location, and/or resistance values are required and these assumptions influence how
756 resistance is calculated and represented in the model. When *a priori* assumptions are made
757 about the importance of resistance values, they must be aggregated to produce an overall
758 resistance value before model-based assessment takes place. This is not the case for
759 resistance covariates, where importance is assessed for each covariate within a model-based
760 framework.

761 Figure 2. A summary of common model types and their ability to meet modeling needs for
762 a typical landscape genetics study.

763 Figure 3. Spatially structured ecological networks contain nodes and edge weights
764 represented in network or matrix format (a). The matrix \mathbf{W} represents edge weights
765 between node pairs, while \mathbf{D}_w is a diagonal matrix containing the sum of the edge weights
766 for each node's first-order neighbors (e.g., $(D_w)_{1,1} = 1 + 4 + 3 = 8$). These two matrices
767 contain information about the conditional structure implied by the edges and is used to
768 generate the precision matrix, \mathbf{Q} , in a conditional autoregressive (CAR) model (b). Two
769 nodes that are conditionally independent in the precision matrix (e.g., $Q_{3,2} = 0$) may still
770 be spatially dependent (i.e., correlated) through intervening nodes (e.g., $\Sigma_{3,2} \neq 0$) in the

771 covariance matrix, $\Sigma = \mathbf{Q}^{-1}$ (c) and the correlation matrix (e). The precision matrix
772 defines the partial correlation among measurements on nodes (d) after accounting for the
773 influence of intervening nodes.

774 Figure 4. Resistance surfaces for the isolation by distance (IBD), isolation by resistance
775 (IBR), and isolation by barrier (IBB) evolutionary-process hypotheses.

776 Figure 5. (a) The isolation-by-resistance (IBR) model ($\mathbf{D}_{\text{IBR}} \sim \text{IBR}$) shows that
777 conductance (inverse resistance) has a non-linear relationship with the IBR resistance
778 covariate (solid black line). The dotted lines denote the 95% confidence intervals. (b)
779 Similar patterns are observed in a map of mean conductance, which is highest in areas with
780 low resistance covariate values.

Author Manuscript

Author Manuscript

Figure 1:

Figure 2:

Author Manuscript

Author Manuscript

Figure 3:

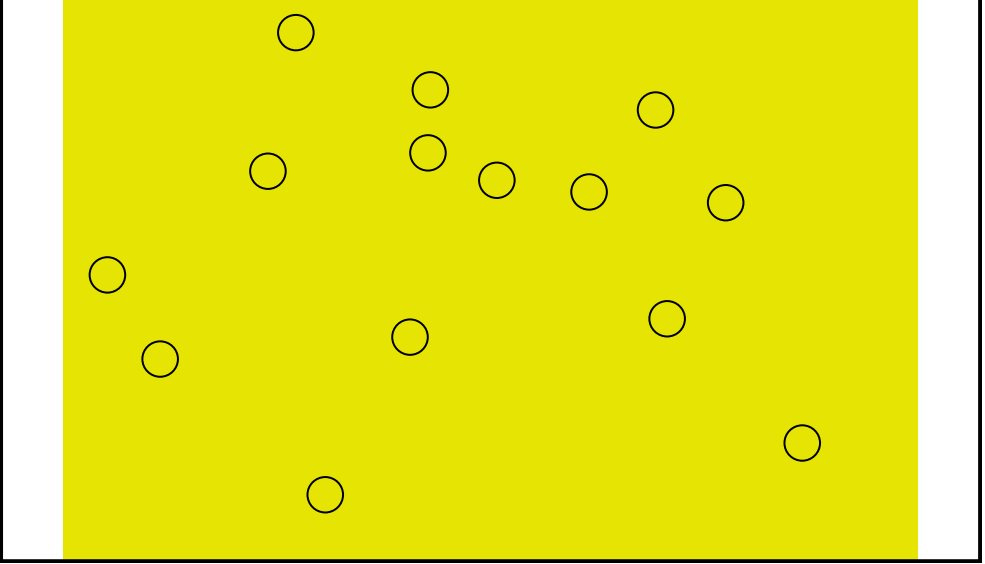
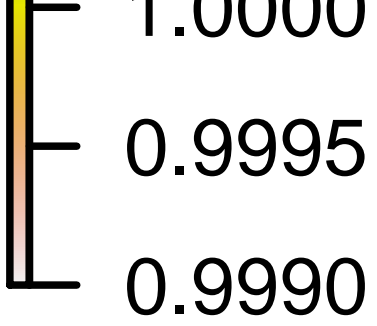
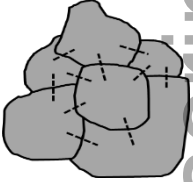
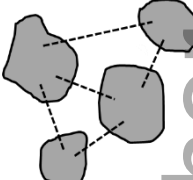


Figure 4:

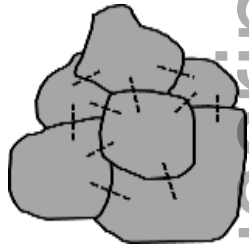
Author Manuscript

Author Manuscript

Figure 5:

Data Format	Resistance Covariates	<i>A priori</i> Assumptions	Assumption-based Outcomes	Resistance Aggregation	Model
Contiguous 	Node-based Size, habitat quality, vegetation cover, distance between centroids	1st Order Neighborhood Structure Rook, Queen, % Shared boundary	Resistance Covariates	None	Model-based Estimates for individual resistance covariates
Non-contiguous 	Node- or/and Edge-based Habitat quality, vegetation cover, distance between node boundaries or centroids	Edge Location Euclidean distance, buffered Euclidean distance	Resistance Covariates		
		Resistance Values Expert opinion, literature review, empirical data, animal movement rates	Edge Location Least-cost path, buffered least-cost path, multiple-least-cost path, Circuit-scape		

Data Format	Resistance Covariates	A priori Assumptions	Assumption-based Outcomes	Resistance Aggregation
-------------	-----------------------	----------------------	---------------------------	------------------------



Node-based

Size, habitat quality, vegetation cover, distance between centroids

1st Order Neighborhood Structure

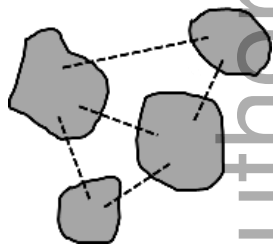
Rook, Queen, % Shared boundary

Edge Location

Euclidean distance, buffered Euclidean distance

Resistance Values

Model estimates



Node- or/and Edge-based

Habitat quality, vegetation cover, distance between node boundaries or centroids

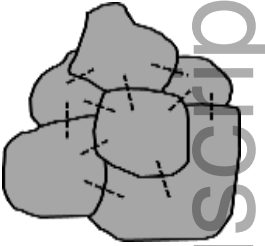
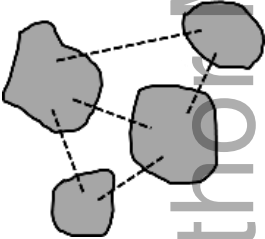
Resistance Values

Expert opinion, literature review, empirical data, rates of animal movement

Edge Location

least-cost path, buffered least-cost path, multiple-least-cost path, Circuit-scape

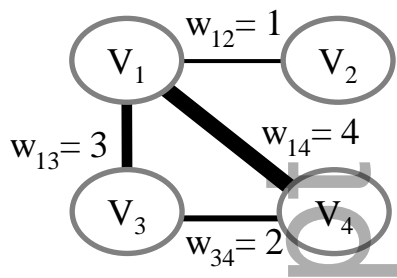
Edge Location + Resistance Values

Data Format	Resistance Covariates	<i>A priori</i> Assumptions	Assumption-based Outcomes	Resistance Aggregation
	Node-based Size, habitat quality, vegetation cover, distance between centroids	1st Order Neighborhood Structure Rook, Queen, % Shared boundary →	Resistance Values Model estimates	
	Node- or/and Edge-based Habitat quality, vegetation cover, distance between node boundaries or centroids ↗ → ↘	Edge Location Euclidean distance, buffered Euclidean distance →	Resistance Values Model estimates	Sum, difference, weighted product, mean, geometric mean, median
Resistance Values Expert opinion, literature review, empirical data, animal movement rates →	Edge Location Least-cost path, buffered least-cost path, multiple-least-cost path, Circuit-scape			
Edge Location + Resistance Values				

Type	Method	Probabilistic Distribution	No <i>a priori</i> Resistance Assumptions	Estimated Resistance Component Parameters	Spatially Correlated Residuals Permitted	Model Selection	Missing Data	Prediction	Sources and Applications
Simulation	Computer simulation	✗	✗	✗	✓	✗	✓	✓	Epperson et al. (2010) Cushman & Landguth (2010)
Matrix Correlation	Mantel/Partial Mantel tests	✗	✗	✗	✗	¹ PT	✗	✗	Mantel (1967), Smouse et al. (1986), Cushman et al. (2006), Legendre & Fortin (2010)
Ordination	Multi-dimensional scaling	✗	✗	✗	✗	¹ PT	✗	✗	Legendre & Legendre (2012), Legendre & Fortin (2010)
	Spatial principle components analysis	✗	✗	✗	✓	¹ PT	✗	✗	Jombart et al. (2008)
	Correspondence analysis, Redundancy analysis, Canonical correlation analysis	✗	✗	✗	✗	¹ PT	✗	✗	ter Braak (1986), Balkenhol et al. (2009), Jombart et al. (2009), Legendre & Fortin (2010), Fortin & Dale (2014)
Regression	Multiple regression on distance matrices	✗	✗	✓	✗	¹ PT	✗	✗	Legendre et al. (1994), Legendre et al. (2015)
	Gravity model: Unconstrained & Singly Constrained	✓	✗	✗	✗	² DA, ITC, CV	✗	✓	Fotheringham & O’Kelly (1989), Murphy et al. (2010), Murphy et al. (2016)
	Spatial Autoregressive model	✓	✓	✓	✓	² DA, ITC, CV	✓	✓	Hanks and Hooten (2013), Ver Hoef et al. (2017)

¹Permutation test (PT), ²Distributional assumptions, Information theoretic criteria, cross-validation (DA, ITC, CV)

Network and Matrix Representation



$$\mathbf{W} = \begin{matrix} & \begin{matrix} V_1 & V_2 & V_3 & V_4 \end{matrix} \\ \begin{matrix} V_1 \\ V_2 \\ V_3 \\ V_4 \end{matrix} & \begin{bmatrix} 0 & 1 & 3 & 4 \\ 1 & 0 & 0 & 0 \\ 3 & 0 & 0 & 2 \\ 4 & 0 & 2 & 0 \end{bmatrix} \end{matrix}$$

$$\mathbf{D}_W = \begin{matrix} & \begin{matrix} V_1 & V_2 & V_3 & V_4 \end{matrix} \\ \begin{matrix} V_1 \\ V_2 \\ V_3 \\ V_4 \end{matrix} & \begin{bmatrix} 8 & 0 & 0 & 0 \\ 0 & 1 & 0 & 0 \\ 0 & 0 & 5 & 0 \\ 0 & 0 & 0 & 6 \end{bmatrix} \end{matrix}$$

(a)

Precision Matrix

$$\mathbf{Q} = (\mathbf{D}_W - \rho \mathbf{W}), \quad \rho = 0.90$$

Covariance Matrix

$$\mathbf{\Sigma} = \mathbf{Q}^{-1}$$

$$\mathbf{Q}_{CAR} = \begin{matrix} & \begin{matrix} V_1 & V_2 & V_3 & V_4 \end{matrix} \\ \begin{matrix} V_1 \\ V_2 \\ V_3 \\ V_4 \end{matrix} & \begin{bmatrix} 8.0 & -0.9 & -2.7 & -3.6 \\ -0.9 & 1.0 & 0 & 0 \\ -2.7 & 0 & 5.0 & -1.8 \\ -3.6 & 0 & -1.8 & 6.0 \end{bmatrix} \end{matrix}$$

$$\mathbf{\Sigma}_{CAR} = \begin{matrix} & \begin{matrix} V_1 & V_2 & V_3 & V_4 \end{matrix} \\ \begin{matrix} V_1 \\ V_2 \\ V_3 \\ V_4 \end{matrix} & \begin{bmatrix} 0.55 & 0.49 & 0.46 & 0.47 \\ 0.49 & 1.44 & 0.42 & 0.42 \\ 0.46 & 0.42 & 0.62 & 0.46 \\ 0.47 & 0.42 & 0.46 & 0.59 \end{bmatrix} \end{matrix}$$

(b)

(c)

Partial Correlation Matrix

$$\mathbf{k}_{i,j|} = \text{corr}(\varepsilon_{i|}, \varepsilon_{j|}) = -\mathbf{Q}_{i,j} / \sqrt{\mathbf{Q}_{i,i} \mathbf{Q}_{j,j}}$$

Correlation Matrix

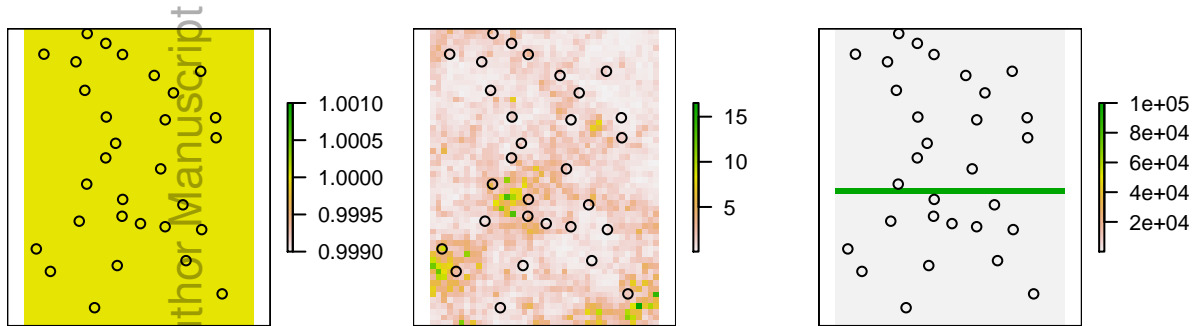
$$\text{Corr}_{i,j} = \mathbf{\Sigma}_{i,j} / \sqrt{\mathbf{\Sigma}_{i,i} \mathbf{\Sigma}_{j,j}}$$

$$\mathbf{k}_{CAR} = \begin{matrix} & \begin{matrix} V_1 & V_2 & V_3 & V_4 \end{matrix} \\ \begin{matrix} V_1 \\ V_2 \\ V_3 \\ V_4 \end{matrix} & \begin{bmatrix} 1 & 0.32 & 0.43 & 0.52 \\ 0.32 & 1 & 0 & 0 \\ 0.43 & 0 & 1 & 0.33 \\ 0.52 & 0 & 0.33 & 1 \end{bmatrix} \end{matrix}$$

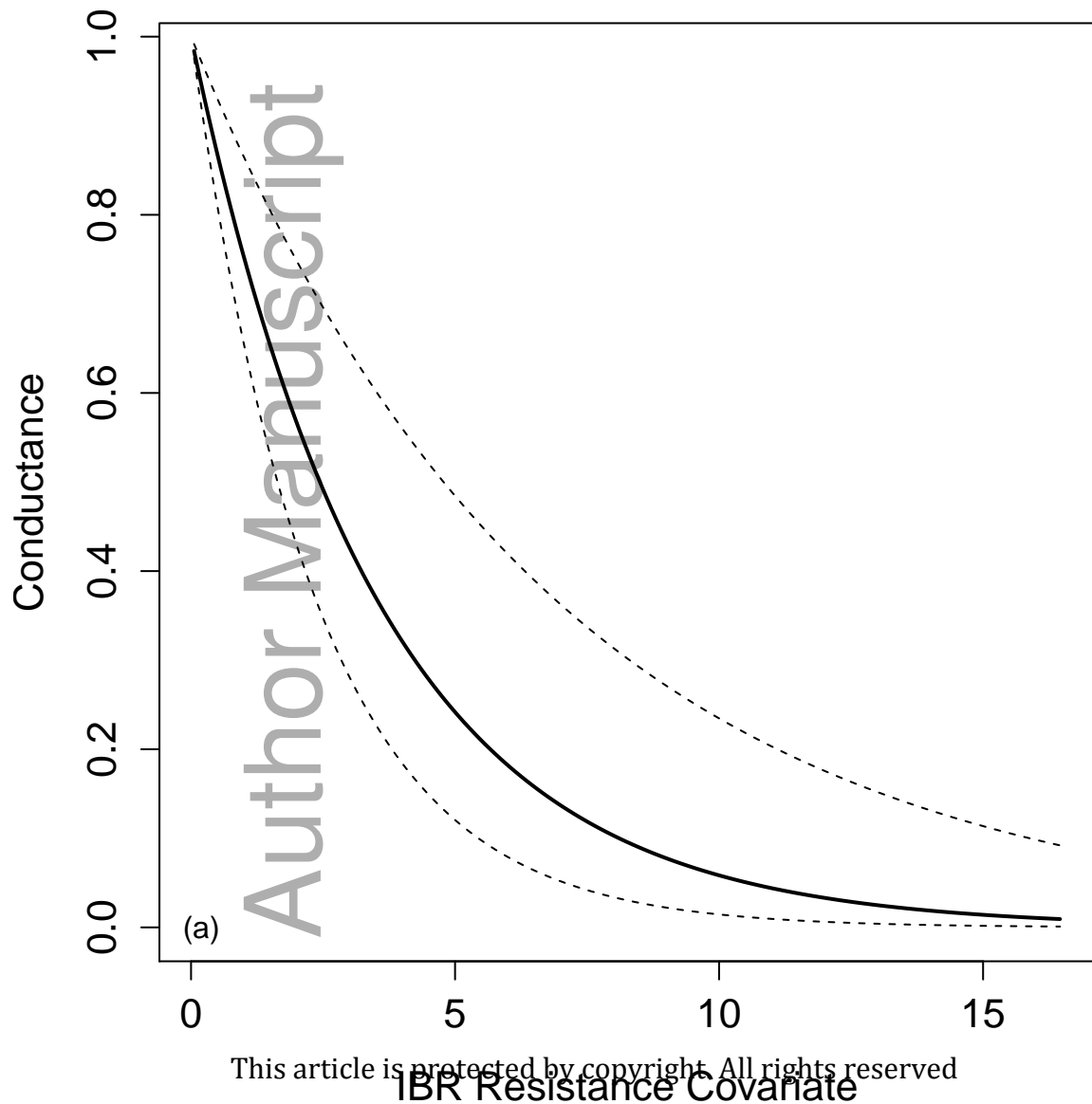
$$\text{Corr}_{CAR} = \begin{matrix} & \begin{matrix} V_1 & V_2 & V_3 & V_4 \end{matrix} \\ \begin{matrix} V_1 \\ V_2 \\ V_3 \\ V_4 \end{matrix} & \begin{bmatrix} 1 & 0.55 & 0.80 & 0.83 \\ 0.55 & 1 & 0.44 & 0.46 \\ 0.80 & 0.44 & 1 & 0.77 \\ 0.83 & 0.46 & 0.77 & 1 \end{bmatrix} \end{matrix}$$

(d)

(e)



Conductance ~ IBR Resistance



Mean Conductance

